PROCEEDINGS OF SCIENCE

Matching and parton-shower accuracy

Ludovic Scyboz[a,*]

[a] *Rudolf Peierls Centre for Theoretical Physics, Clarendon Laboratory, Parks Road, Oxford OX1 3PU, UK*

E-mail: ludovic.scyboz@physics.ox.ac.uk

In this talk I investigate the interplay of NLO matching and next-to-leading-logarithmic (NLL) parton showers in the context of two-body decays. Three matching schemes have been implemented in the NLL-accurate PanScales showers: a multiplicative scheme, MC@NLO and POWHEG. By means of both analytic and numerical arguments, I show how these retain the showers NLL accuracy, and (under certain provisions in the case of POWHEG) can augment it so that it achieves NNDL accuracy for global event shapes. The talk also briefly explores some phenomenological considerations.

16th International Symposium on Radiative Corrections: Applications of Quantum Field Theory to Phenomenology (RADCOR2023)
28th May - 2nd June, 2023
Crieff, Scotland, UK

*Speaker

PoS(RADCOR2023)066

1. Introduction

Nowadays Monte-Carlo event generators typically feature automatic matching of parton showers to next-to-leading-order (NLO) matrix elements. While these procedures have been devised a long time ago, we focus here on their interplay with the logarithmic accuracy of the parton shower. More precisely, we investigate the effect of three NLO matching schemes on the logarithmic structure of the NLL-accurate PanScales showers [1, 2], for the simple cases of $\gamma^* \to q\bar{q}$ and $H \to gg$ decays: POWHEG [3, 4] and MC@NLO [5] matching, as well as a multiplicative scheme (internal matrix-element correction for the first shower emission). Ideally, the matching schemes should retain the NLL accuracy of the showers; additionally, if performed correctly, we expect NLO matching to augment that accuracy, and provide next-to-next-to-double-logarithmic (NNDL) accuracy for the 2-jet rate and for global event-shape observables.

2. POWHEG matching

Multiplicative and MC@NLO matching straightforwardly achieve NNDL accuracy for global event shapes, essentially because these two schemes do not modify the structure of shower emissions when they are soft and/or collinear (i.e. deep in the infrared region). Details of the implementation of the two schemes in the PanScales framework, as well as numerical evidence for NNDL accuracy, are provided in Ref. [6].

In contrast, within POWHEG matching, the first emission is always handled externally by a so-called "hardest emission generator" (HEG). As we will show, the handover to the parton shower needs to be performed with care in order to reach NNDL accuracy. Schematically, the POWHEG matching procedure is defined by the following formula:

$$\mathrm{d}\sigma = \bar{B}(\Phi_\mathrm{B})\, S_\mathrm{HEG}(v_\Phi^\mathrm{HEG}, \Phi_\mathrm{B}) \times \frac{R(\Phi)}{B_0(\Phi_\mathrm{B})}\,\mathrm{d}\Phi \times I_\mathrm{PS}(v_\Phi^\mathrm{HEG}, \Phi)\,, \tag{1}$$

where v_Φ^HEG is the value of the ordering variable that corresponds to the phase-space point Φ for the HEG. The normalisation factor $\bar{B}$ is given by

$$\bar{B}(\Phi_\mathrm{B}) = B_0(\Phi_\mathrm{B}) + V(\Phi_\mathrm{B}) + \int R(\Phi)\mathrm{d}\Phi_\mathrm{rad}\,, \tag{2}$$

with $B_0(\Phi_\mathrm{B})$ the Born squared matrix element, $V(\Phi_\mathrm{B})$ the virtual 1-loop contribution, and $R(\Phi)$ the real emission squared matrix element. The Sudakov form factor in Eq. (1) is

$$S_\mathrm{HEG}(v, \Phi_\mathrm{B}) = \exp\left[-\int_{v_\Phi^\mathrm{HEG} > v} \frac{R(\Phi)}{B_0(\Phi_\mathrm{B})}\mathrm{d}\Phi_\mathrm{rad}\right], \tag{3}$$

and $I_\mathrm{PS}(v_\Phi^\mathrm{HEG}, \Phi)$ represents symbolically the iteration of shower emissions from v_Φ^HEG down to the shower cutoff.

One comment about the choice of ordering variable is in order: in the standard `POWHEG-BOX` implementation with transverse-momentum ordered showers ($\beta_\mathrm{PS} = 0$ in a PanScales parameterisation [2]), the ordering variables at a given phase-space point Φ, v_Φ^HEG and v_Φ^PS, coincide when the emission is soft and collinear. This is crucial in order to retain the leading-logarithmic accuracy of

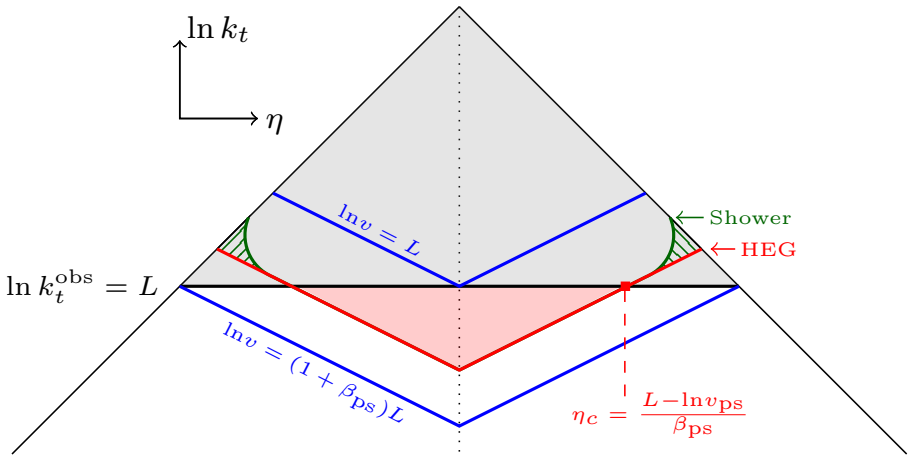

Figure 1: Lund plane [8] illustration of a kinematic mismatch in the hard-collinear region between the contours of $v^{\rm HEG}$ for the HEG's ordering variable (in red), and the parton shower's $v^{\rm PS}$ (in green). The constraint on the observable is a flat contour ($\beta_{\rm obs} = 0$, in black).

the shower. In the case of the PanScales showers, where we do not necessarily restrict ourselves to transverse-momentum ordering ($\beta_{\rm PS} > 0$), we use a generalised version of the Frixione-Kunzst-Signer (FKS) map [7] that satisfies the same requirement, which we will call POWHEG$_\beta$.[1]

2.1 Kinematic mismatches

Nevertheless, the contours of fixed v might still differ in other regions of phase space (for instance when the emission is hard and collinear). This mis-alignment can spoil the expected NNDL accuracy of the matched parton shower. To support this statement with an analytic argument, let us consider the case of the PanLocal shower with $\beta_{\rm PS} > 0$ (where the first matched emission is handled by the HEG, with $\beta_{\rm HEG} = \beta_{\rm PS}$), and an observable with $\beta_{\rm obs} = 0$ (such as the Cambridge $\sqrt{y_{23}}$ 3-jet resolution scale). This situation is depicted in Fig. 1 for the example of the PanLocal shower.

Once the first (matched) emission at Φ is performed by the HEG, we hand over to the PanLocal shower with a starting scale $v_\Phi^{\rm HEG}$, as in Eq. (1). Clearly, part of the phase space is double-counted (see the green shaded triangles in Fig. 1). In double-logarithmic counting, we expect the probability for the observable O to be below some threshold e^L, to be $\Sigma(O < e^L) = e^{-\bar\alpha L^2}$. We find that if the red and green contours do not match in the hard-collinear region, this is instead

$$\Sigma(O < e^L) = e^{-\bar\alpha L^2}\left[1 + 2(e^{-\bar\alpha\beta_{\rm PS}L^2} - 1)\bar\alpha\Delta + O(\mathrm{N^3DL})\right]. \tag{4}$$

Thus the presence of an extra factor (proportional to a term Δ) spoils the result at the NNDL level. For the kinematic mismatch illustrated in Fig. 1, the factor Δ represents the effective size of the mismatch region in the Lund plane (green shaded triangles). In the case of POWHEG as HEG in conjunction with the PanLocal shower, for instance, we can evaluate this factor analytically, and find

$$\bar\alpha\Delta = \bar\alpha\Delta_{\rm kin} = \frac{2C_F\alpha_s}{\pi}\cdot\frac{4\pi^2 - 15}{24}. \tag{5}$$

[1]The generalised kinematic map is given in detail in Appendix C of Ref. [6]

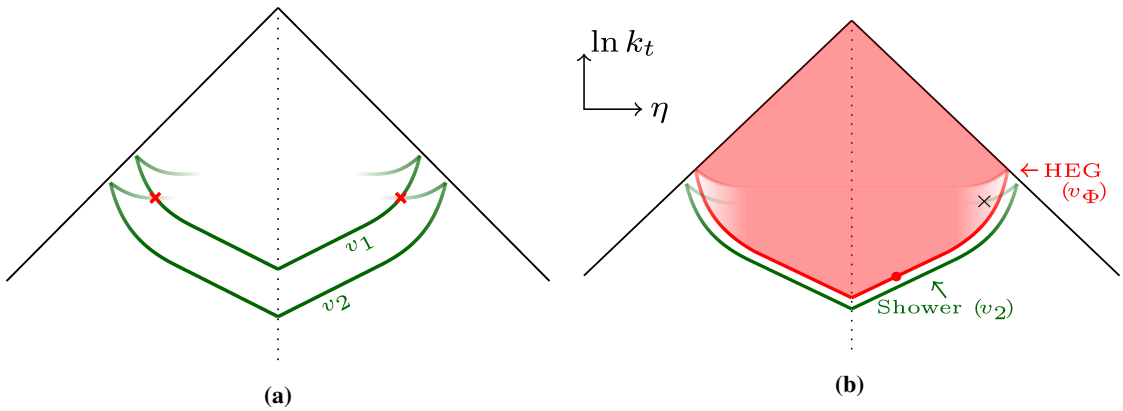

Figure 2: Schematic illustration of the issue associated with gluon asymmetrisation. (a) For a Born gluon splitting to gg or $q\bar{q}$, a given physical point X in the Lund plane (marked with a red cross) can be reached with two different values of the ordering variable v. (b) Because two different values of v contribute to the (non-)emission probability down to a given point, part of the Sudakov at a given physical phase-space point (the black cross, for instance) has not been accounted for after the HEG's first emission (the red curve). A second contribution is supposed to be generated by the parton shower: if the de-symmetrisation parameter is different in the HEG and in the shower, the full contribution is not generated correctly.

As already identified e.g. in Refs. [3, 9], kinematic mismatches between the definition of the ordering variable of the HEG, versus that of the parton shower, can be corrected by vetoing shower emissions in regions already covered by the HEG (e.g. in the green shaded triangles of Fig. 1). Vetoing of shower emissions in those regions restores NNDL accuracy (see numerical tests in Section 3).

2.2 Partitioning mismatch in gluon splitting function

A second subtlety arises with the use of POWHEG matching if gluons are present in the Born event. The issue appears because parton showers (as well as the FKS map in POWHEG, for example) typically partition the full $g \to gg$ splitting function,

$$\frac{1}{2!}P_{gg}(\zeta) = C_A\left(\frac{\zeta}{1-\zeta} + \frac{1-\zeta}{\zeta} + \zeta(1-\zeta)\right), \tag{6}$$

such that there is only one divergence when the emitted gluon becomes soft ($\zeta \to 1$), breaking the symmetry in the momentum fraction $\zeta \leftrightarrow 1-\zeta$. In PanScales, for instance, the de-symmetrised splitting function takes the form:

$$\frac{1}{2!}P^{\text{asym}}_{gg}(\zeta) = C_A\left[\frac{1+\zeta^3}{1-\zeta} + (2\zeta-1)w_{gg}\right], \tag{7}$$

where the parameter w_{gg} fixes the shuffling of finite terms between one singular region and the other. The full splitting function is recovered in the sum, $\frac{1}{2}(P^{\text{asym}}_{gg}(\zeta) + P^{\text{asym}}_{gg}(1-\zeta)) = P_{gg}(\zeta)$.

A NNDL failure similar to that of Section 2.1 arises if the HEG does not de-symmetrise the gluon splitting function in the same manner as the parton shower. The situation is depicted on the Lund plane of Fig. 2. As illustrated here, a given physical phase-space point (marked by a red cross)

can be reached by contours with two different values of the ordering variable, v_1 (on the diagonal branch corresponding to a value of $\zeta > 1/2$) and v_2 (on the flattening branch, corresponding to $\zeta < 1/2$). The total radiation intensity (normalised to 1 for the purpose of illustration) is given by the sum of two contributions, whose relative values depend on how the splitting function was de-symmetrised:

$$1 = f_{X,1}(w_{gg}) + f_{X,2}(w_{gg})\,. \tag{8}$$

In the case of a combination of HEG and shower, as shown in Fig. 2b, a certain fraction of the Sudakov $f_{X,1}(w_{gg}^{\text{HEG}})$ has been accounted for by the HEG. The second contribution, $f_{X,2}(w_{gg}^{\text{PS}})$, is the responsibility of the parton shower: if the de-symmetrisation parameter of the HEG is identical to that of the shower, $w_{gg}^{\text{HEG}} = w_{gg}^{\text{PS}}$, then the two fractions correctly add up to one. If not, the situation is similar to that of a double-counting or a hole in phase space, as for the kinematic mismatch issue presented in Section 2.1.[2]

We find that the impact of such a de-symmetrisation mismatch on the logarithmic structure of an observable (with $\beta_{\text{obs}} < \beta_{\text{PS}}$) is identical to Eq. (4), at NNDL. We derived the mismatch factor $\bar{\alpha}\Delta$ analytically, and find for the PanScales showers:

$$\bar{\alpha}\Delta = \bar{\alpha}\Delta^{\text{PanGlobal}}_{\text{de-symm.}} = \left[(w^{\text{HEG}} - w^{\text{PS}})\left(C_A - n_f T_R\right)\right]\frac{-1}{1+\beta_{\text{PS}}}\,, \tag{9a}$$

$$\bar{\alpha}\Delta = \bar{\alpha}\Delta^{\text{PanLocal}}_{\text{de-symm.}} = \left[(w^{\text{HEG}} - w^{\text{PS}})\left(C_A - n_f T_R\right)\right]\frac{\beta_{\text{PS}}}{1+\beta_{\text{PS}}}\,. \tag{9b}$$

Note that the NNDL discrepancy vanishes exactly for $n_f = 6$. In the numerical tests of Section 3, we will show the expected discrepancy for $n_f = 0$ (to avoid the artificial partial cancellation for $n_f = 5$).

As a final comment, both the kinematic and the de-symmetrisation mismatches generate extra terms that effectively *break* the property of exponentiation. A more complete analysis (in particular for the SoftDrop cross section) can be found in Section 3.1 of Ref. [6].

3. NNDL accuracy tests

Following a similar line of tests as in earlier PanScales work, we consider the probability for an event-shape observable to be smaller than e^L, $\Sigma(\alpha_s, L) = \Sigma(O < e^L)$. To be considered accurate at NNDL, the parton-shower prediction for the cumulative distribution of the observable, Σ_{PS}, must satisfy

$$\delta_{\text{NNDL}} = \lim_{\substack{\alpha_s\to 0\\ \xi \text{ fixed}}} \frac{\Sigma_{\text{PS}}(\alpha_s, -\sqrt{\xi/\alpha_s}) - \Sigma_{\text{NNDL}}(\alpha_s, -\sqrt{\xi/\alpha_s})}{\alpha_s \Sigma_{\text{DL}}} = 0\,, \tag{10}$$

with $\xi = \alpha_s L^2$. Details about the extrapolation procedure are given in Ref. [6]. In Fig. 3, the quantity δ_{NNDL} is plotted on the x-axis, for the PanLocal showers (dipole and antenna, with $\beta_{\text{PS}} = \frac{1}{2}$), as well as for the PanGlobal shower (with $\beta_{\text{PS}} = 0, \frac{1}{2}$), without any 3-jet matching, for a set of global event shapes (categorised by their values of $\beta_{\text{obs}} = 0, \frac{1}{2}, 1$). The uncertainty bands are defined as a combination of the statistical uncertainty, as well as a systematic uncertainty from the extrapolation

[2] In PanScales we also use a de-symmetrisation factor w_{qg} for the $g \to q\bar{q}$ splitting function. In the following we will always choose $w = w_{gg} = w_{qg}$

$\alpha_s \to 0$, added linearly. As is evident from Fig. 3, the pure showers are not NNDL-accurate, and the discrepancy at NNDL is roughly of order $O(1)$.

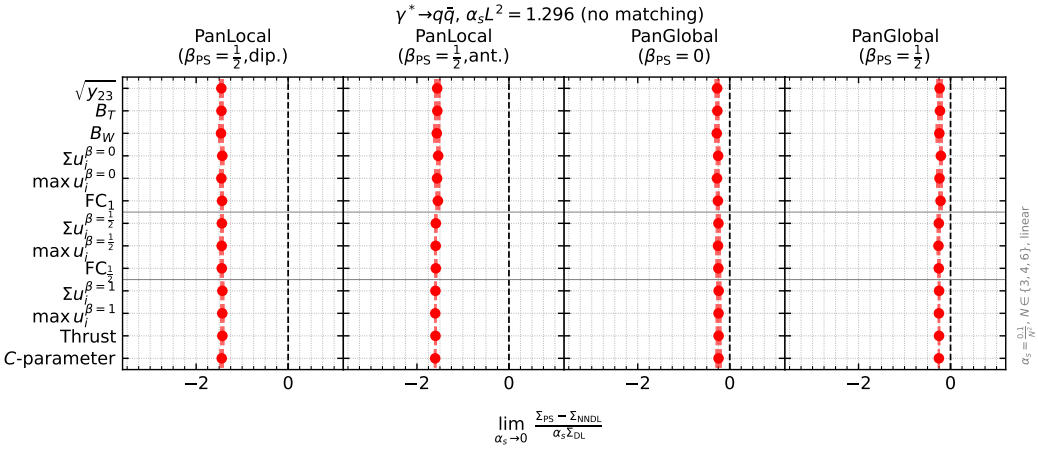

Figure 3: Results of the NNDL accuracy tests at fixed $\xi = \alpha_s L^2$ for the NLL-accurate PanScales showers, without 3-jet matching, for $\gamma^* \to q\bar{q}$.

Next, we consider POWHEG-style matching, using PanGlobal as the HEG (with $\beta_{PS} = \frac{1}{2}$), or POWHEG$_\beta$, matched to either PanGlobal ($\beta_{PS} = 0, \frac{1}{2}$) or the PanLocal shower ($\beta_{PS} = \frac{1}{2}$). Where it is required we apply the kinematic veto discussed in Section 2.1, and we align the choice of de-symmetrisation parameter between the HEG and the shower, as explained in Section 2.2. With

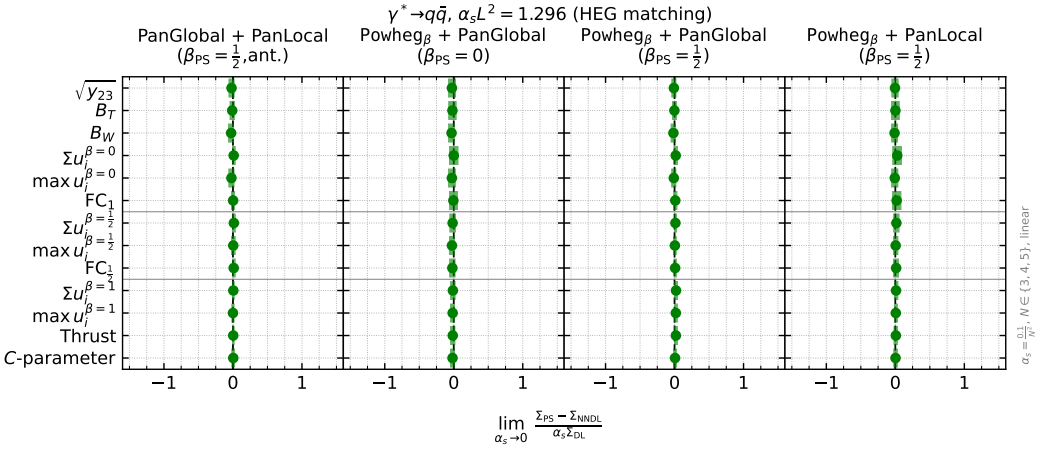

Figure 4: Results of the NNDL accuracy tests for four HEG/shower combinations, for $\gamma^* \to q\bar{q}$. Matched results are similar for $H \to gg$, as well as for the MC@NLO and multiplicative matching schemes. The corresponding plots can be found in Ref. [6].

3-jet matching enabled, we find agreement for all combinations of HEG/shower and observables at NNDL accuracy (the results for $\gamma^* \to q\bar{q}$ are shown in Fig. 4).

Finally, we compare the size of the NNDL discrepancy to the expectation computed in Sections 2.1, 2.2, in cases of a kinematic mismatch that remains uncorrected by the application of the veto (for $\gamma^* \to q\bar{q}$, Fig. 5a), or where the de-symmetrisation parameter for the gluon splitting

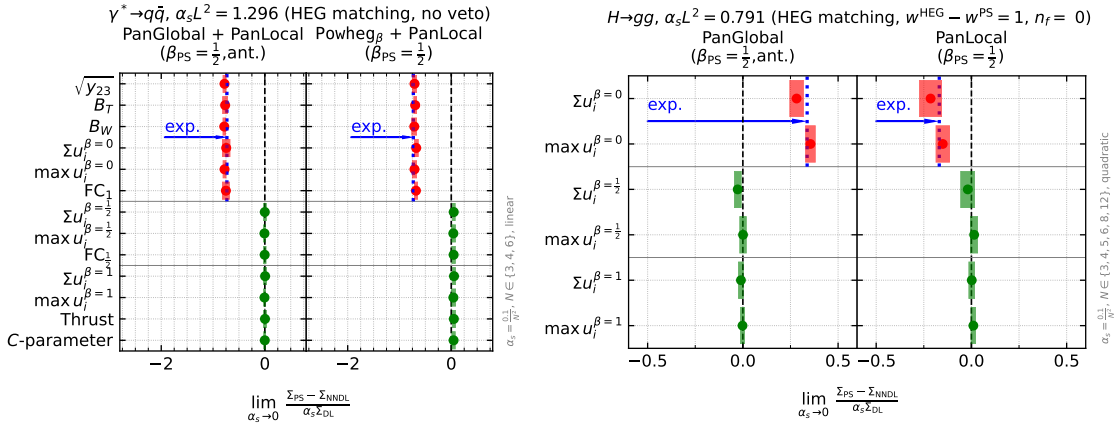

(a) **(b)**

Figure 5: Results of the NNDL accuracy tests (a) for PanGlobal and POWHEG$_\beta$ (as HEG) in conjunction with PanLocal (both with $\beta_{PS} = \frac{1}{2}$), without the kinematic veto needed in hard-collinear regions, and (b) for PanGlobal and PanLocal, where we use the same shower as HEG and for subsequent emissions, but where the de-symmetrisation parameters of the gluon splitting functions are left mis-aligned, $w^{HEG} \neq w^{PS}$.

function is purposefully left mis-aligned (for $H \to gg$, Fig. 5b). As predicted, NNDL tests fail for observables with $\beta_{obs} < \beta_{PS}$, and the size of the observed NNDL discrepancy for $\beta_{obs} = 0$ agrees with the values computed from Eqs. (5), (9), shown as a dotted blue line (marked "exp.").

4. Phenomenology

Finally, we consider several matched showers in a physical context. Fig. 6 shows parton-level distributions for the thrust $1 - T$ at $\sqrt{s} = m_Z$ (top panels) and for a SoftDrop $\ln k_T/Q$ distribution at $\sqrt{s} = 2$ TeV (with $z_{cut} = 0.25$ and $\beta_{SD} = 0$, bottom panels). These plots feature our own implementation of the Pythia 8 shower [10] (PSPythia8, leftmost column), the PanGlobal shower ($\beta_{PS} = 0$, middle column) and the PanLocal dipole shower ($\beta_{PS} = \frac{1}{2}$, rightmost column); unmatched showers are depicted in red, correctly-matched showers in blue, and the Powheg-matched PanLocal shower without a proper kinematic veto, see Section 2.1, in green. The smaller panels show the ratio of these curves to the PanGlobal $\beta_{PS} = 0$ shower matched with the multiplicative scheme.

We also estimate scale uncertainties as an envelope of renormalisation scale variations (dashed lines) and an uncertainty coming from shower emissions beyond the first, matched emission in the hard region (dotted lines). Details can be found in Ref. [6]. The three main conclusions are that (1) matched showers broadly agree in their central values within the uncertainty bands, (2) NLL-accurate showers come with a much-reduced uncertainty band (by a factor ~ 2 in comparison with a LL-accurate shower) and (3) in particular in the case of the SoftDrop observable, the NNDL-breaking effect of the hard-collinear kinematic mismatch (green, `no-veto`) drives the curve significantly away from the correct result for moderately large values of the logarithm L.

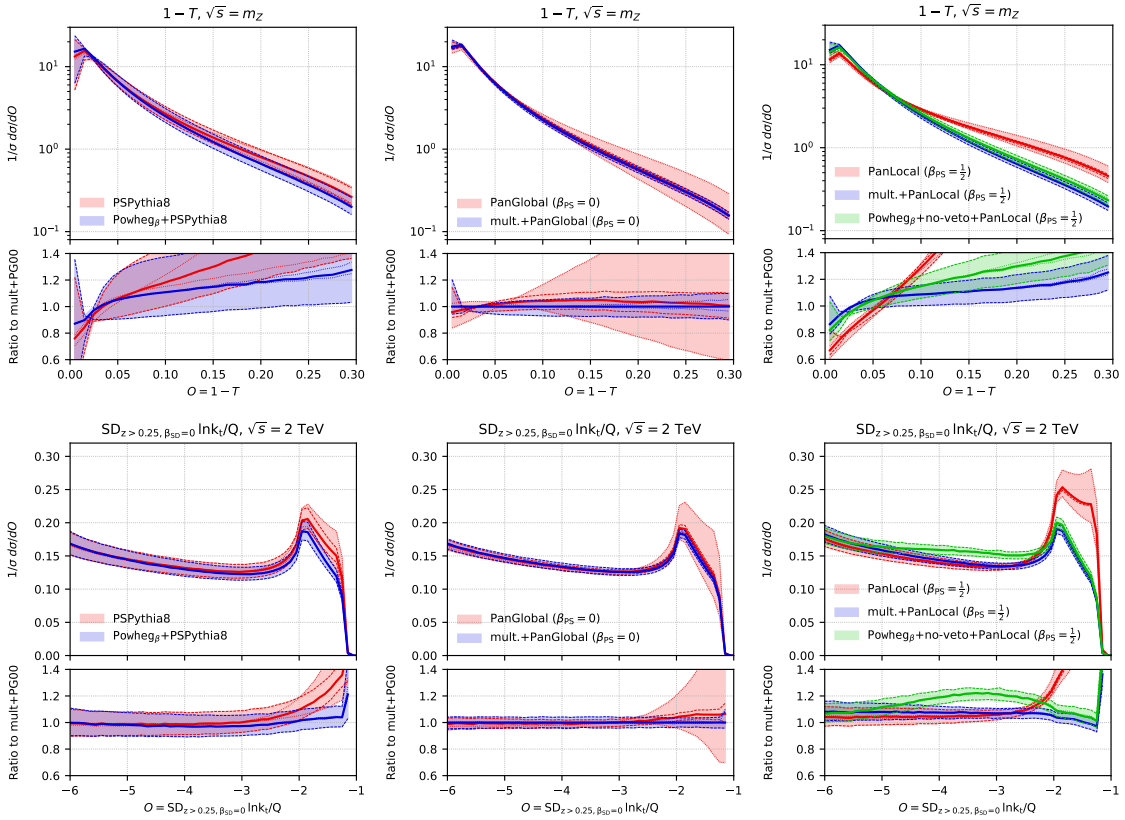

Figure 6: Thrust (top) and SoftDrop $\ln k_t/Q$ (bottom) distributions, unmatched (red) and matched (blue), for our PanScales implementation of the Pythia 8 shower (PSPythia 8 , left)) and two NLL showers: PanGlobal with $\beta_{\text{PS}} = 0$ (middle column) and PanLocal $\beta_{\text{PS}} = \frac{1}{2}$ (right).

5. Conclusions

We have investigated the interplay of NLO matching and parton-shower accuracy in the context of simple two-body decays. The conclusion, namely that NLO matching can augment the NLL accuracy of the shower to achieve NNDL accuracy for global event shapes, holds straightforwardly for MC@NLO and our internal shower matrix-element correction. In the case of POWHEG, we found that a careful alignment of the HEG and parton-shower contours is needed, not only in the soft-collinear region, but also e.g. in the hard-collinear edges of phase space. A related issue arises when two different contours contribute to the same phase-space point, such as when gluons are present in the Born event. With the help of both analytic and numerical arguments, we have shown that these kinematic and de-symmetrisation mismatches spoil the accuracy of the matched shower at NNDL level (in fact, they even break the property of exponentiation more fundamentally).

We have also taken preliminary steps in the investigation of phenomenological results, and observed a significant reduction of systematic uncertainties coming from the use of NLL-accurate showers. These conclusions will be expanded upon in future work with the inclusion of further higher-logarithmic contributions (NNLL), massive quarks, hadronisation/MPI and a proper tune of the PanScales showers.

References

[1] M. Dasgupta, F. A. Dreyer, K. Hamilton, P. F. Monni and G. P. Salam, *Logarithmic accuracy of parton showers: a xed-order study*, JHEP 09 (2018) 033, [1805.09327]

[2] M. Dasgupta, F. A. Dreyer, K. Hamilton, P. F. Monni, G. P. Salam and G. Soyez, *Parton showers beyond leading logarithmic accuracy*, Phys. Rev. Lett. 125 (2020) 052002, [2002.11114]

[3] P. Nason, *A New method for combining NLO QCD with shower Monte Carlo algorithms*, JHEP 11 (2004) 040, [hep-ph/0409146]

[4] S. Frixione, P. Nason and C. Oleari, *Matching NLO QCD computations with Parton Shower simulations: the POWHEG method*, JHEP 11 (2007) 070, [0709.2092]

[5] S. Frixione and B. R. Webber, *Matching NLO QCD computations and parton shower simulations*, JHEP 06 (2002) 029, [hep-ph/0204244]

[6] K. Hamilton, A. Karlberg, G. P. Salam, L. Scyboz, and R. Verheyen, *Matching and event-shape NNDL accuracy*, JHEP 03 (2023) 224, [2301.09645]

[7] S. Frixione, Z. Kunszt and A. Signer, *Three jet cross-sections to next-to-leading order*, Nucl. Phys. B 467 (1996) 399442, [hep-ph/9512328]

[8] B. Andersson, G. Gustafson, L. Lonnblad and U. Pettersson, *Coherence Effects in Deep Inelastic Scattering*, Z. Phys. C43 (1989) 625

[9] R. Corke and T. Sjostrand, *Improved Parton Showers at Large Transverse Momenta*, Eur. Phys. J. C 69 (2010) 118, [1003.2384]

[10] T. Sjostrand and P. Z. Skands, *Transverse-momentum-ordered showers and interleaved multiple interactions*, Eur. Phys. J. C39 (2005) 129154, [hep-ph/0408302]